Qualitative and quantitative assessment of water sorption in natural fibres using ATR-FTIR spectroscopy

Amandine Célino, Olivier Gonçalves, Frédéric Jacquemin, Sylvain Fréour

Qualitative and quantitative assessment of water sorption in natural fibres using ATR-FTIR spectroscopy

A. Célino[1]*, O. Gonçalves [2] F. Jacquemin[1], S. Fréour[1]

[1] Institut de Recherche en Génie Civil et Mécanique, UMR CNRS 6183, 37 Boulevard de l'Université, 44602 Saint-Nazaire Cedex, France,
[2] GEPEA, UMR CNRS 6144, 37 Boulevard de l'Université, 44602 Saint-Nazaire Cedex, France

*Corresponding author: Amandine Célino

GeM, UMR CNRS 6183

37 Boulevard de l'Université, BP 406

44602 Saint-Nazaire Cedex

Telephone number: +33240172625

Fax number: +33240172618

E-mail address: amandine.celino@univ-nantes.fr

Abstract

In the field of composite materials, natural fibres appear to be a viable replacement for glass fibres. However, in humid conditions, strong hydrophilic behavior of such materials can lead to their structural modification. Then, understanding moisture sorption mechanisms in these materials is an important issue for their efficient use . In this work, the water sorption on three natural fibres (flax, hemp and sisal) was studied using Fourier Transformed InfraRed spectroscopy. The spectral informations allowed both qualitative and quantitative analysis of the moisture absorption mechanisms. The main chemical functions involved in the water sorption phenomenon were identified. The absolute water content of the fibres was also determined by using a Partial Least Square Regression (PLS-R) approach. Moreover, typical sorption isotherm curves described by Park model were fitted as well as water diffusion kinetics These last applications confirmed the validity of the FTIR spectra based predictive models.

Keywords*: natural fibres, water sorption, Fourier Transformed InfraRed spectroscopy, Partial Least Square Regression, diffusion kinetics*

1. Introduction

Nowadays, natural fibres are considered to be a good alternative for glass fibres replacement in the purpose of composite material reinforcement (particularly in automotive manufacturing or sport and leisure sector) (Bledzki & Gassan, 1999; Suddell & Evans, 2005). These fibres

present a better environmental impact than glass fibres (recyclability, biodegradability) as well as higher specific mechanical properties because of their low density. However, their pronounced hydrophilic behavior -due to their particular structure- leads to high level of moisture absorption in wet environments (Célino, Fréour, Jacquemin, & Casari, 2013). This results in the structural modification of the fibres and an evolution of their mechanical properties together with the composites in which they are fitted in (Dakhal, Zhan, & Richardson, 2007; Placet, Cisse, & Boubakar, 2012; Symington, Banks, David, & Pethrick, 2009). Thereby, the understanding of these moisture absorption mechanisms is of great interest to get a better control of such new biomaterials.

Generally, one of the most important factors controlling the water diffusion phenomenon in polymeric materials is the molecular interaction occurring between the diffusing compound and the substrate. The diffusion phenomenon is subjected to the ability of the polymer molecular sites to establish hydrogen bonds with the water molecules. Spectroscopic techniques such as Nuclear Magnetic Resonance (NMR), dielectric or Fourier Transform Infra-Red spectroscopy (FTIR) have been proved to be well adapted to study this phenomenon since they allow to characterize molecular interactions involving potential sorption sites for water (Mijovic & Zhang, 2003; Popineau, Rondeau-Mouro, Suplice-Gaillet & Martin, 2005). Among these approaches, FTIR spectroscopy has been widely used to study water transport in polymer and particularly to study the water sorbed into epoxy resins (Cotugno, Larobina, Mensitieri, Musto & Ragosta, 2001; Feng, Berger, & Douglas, 2004; Fieldson & Barbari, 1993; Musto, Ragosta, & Mascia, 2000). Indeed, this technique provides attractive features: i.e. the very high sampling rate, the sensitivity, the accuracy of the quantitative analysis and the informations at the molecular level contained in the vibrational spectra. Moreover, the development of Attenuated Total Reflectance FTIR spectroscopy (ATR-FTIR) encouraged and facilitated the use of this non-invasive technique directly onto solid materials (Chalmers & Dent, 1997).

On pure cellulosic polymers, the potential sorption sites for water were determined to be hydroxyl and carboxyl groups which are particularly easily detected in FTIR spectroscopy (Berthold, Olsson, & Salmén, 1998). However, few studies have been performed to characterize water sorption by FTIR directly on raw lignocellulosic fibres. (Laity & Hay, 2000) demonstrated that it was possible to reproduce water sorption kinetics by recording infrared spectra in reflexion mode on cellophane. More recently, (Olsson & Salmén, 2004) examined the association of water on pulp paper using FTIR spectra acquired in transmission mode. Their results indicated the existence of characteristic bands affected by water. Moreover they determined a linear relationship between the absorbance of those bands and the water content, using a univariate approach. This last work was of particular importance since it highlighted major features helping the understanding of chemical groups involved in water diffusion in pulp paper. However both approaches, based on univariate analysis of FTIR signal failed to properly reproduce the sorption isotherms.

The aim of this work is the use of FTIR as an experimental tool to investigate the water sorption onto raw plant fibres, known to be good candidates for the reinforcement of

composite materials (i.e. flax, hemp and sisal). First FTIR spectral signature of each fibre was investigated in order to describe the molecular effect of the water sorption mechanisms. Secondly, a multivariate model linking water sorption and the whole FTIR spectra was developed using partial least square regression (PLS-R). Finally this model was applied for the accurate monitoring of the water diffusion in the tested biomaterials.

2. Materials and methods

2.1 Materials

Among the disposable plant fibres, hemp, flax, and sisal fibres were chosen because they presented the best mechanical properties regarding the replacement of glass fibres for the purpose of reinforcing the polymeric matrix (Summerscales, Dyssanayake, Virk & Hall, 2010; Wambua, Ivens, & Verpoest, 2003,). In our study, the bundle of the model fibres was investigated. Bundle of fibres are extracted from the stem (flax and hemp) or the leaf (sisal) of the plant. They are composed of about ten elementary fibres linked together by a pectic cement (i.e. the middle lamella). Their section is in the order of a few millimeters.

2.2 Moisture sorption protocol

First, all thefibre samples tested were dried in desiccators containing silicate gel for 48 hours before controlled moisture sorption treatment. Then, samples were placed in different hygroscopic conditions in a climatic chamber (supplied by Climats and assisted by Spiral 3 software) in order to get samples with different water content. The relative humidities tested were 30, 50, 60, 75, 85 and 97 % at room temperature. Experimental sorption isotherms and sorption kinetics were obtained by periodically weighting the samples. Dynamic Vapour Sorption apparatus could also been used to plot sorption isotherms with more accuracy as demonstrated by (Bessadok et al., 2009 or Xie et al., 2011). But in our case, gravimetric measurement provided necessary results. Data were read to 0.01 mg on a precision balance (Sartorius – MC1 Analytic AC210P). The equilibrium moisture content Ms is considered to be reached when the mass is stable according to relation (1).

$$M_W(\%) = \frac{M(t) - M_0}{M_0} \times 100 \quad (1)$$

where M_0 is the initial weight of the bulk specimens before moisture sorption (dry conditions) and M(t) is the weight of the specimen at time t.

2.3 Infrared spectroscopic investigations

2.3.1 ATR-FTIR spectra acquisition

Infrared spectra were recorded in reflection mode directly on the single reflexion diamond crystal of the ATR accessory loaded with bundles of the three fibres presented in section 2.1. The Bruker tensor 27 FTIR spectrometer equipped with the ATR platinum module, with a deuterated triglycine sulphate detector RT-DLaTGS and the OPUSv7.0.122 software (Bruker Optics, Germany) was set up with the following parameters. The spectral resolution was fixed

to 1 cm^{-1}, the number of scans to 32, the selected spectral range between 4000 and 400 cm^{-1}. The penetration depth in the fibres was 0.4 µm at 4000 cm^{-1} and 2.7 µm at 600 cm^{-1} according to equation (2) relating penetration depth (dp) to wavelength.

$$dp = \frac{\lambda}{2\Pi n_1 \sqrt{\sin^2\theta - (n_2/n_1)^2}} \quad (2)$$

Where λ is the infrared wavelength, n_1, the refractive index of the internal reflexion element (IRE), n_2 the refractive index of the substrate and θ the angle of incidence of the IR beam (Griffith & Haseth, 2007). In our case n_1= 2.41, n_2=1.5 for the fibres assimilated as polymer, θ = 40 °, and λ = 4000-600 cm^{-1}).

Background spectra were collected using the same instrument settings as those employed for the samples and was performed against air. Spectra were recorded for 10 replicates per fibre sample.

2.3.2 ATR-FTIR spectra acquisition in kinetic mode

For the monitoring of water diffusion, time dependent ATR-FTIR spectra were acquired every 2 minutes in ambient conditions during drying of a saturated fibre sample. Each tested fibres were systematically placed in a relative humidity atmosphere of 95 % before the measurement. Recorded spectra were directly treated by Partial Least Square regression (section 2.3.4) in order to determine the water content and to plot the drying kinetics of the tested fibres. Then, the results were compared with the kinetics obtained by the gravimetric measurements. For the gravimetric measurements, the samples were placed on a precision balance (0.01 mg) during the drying step and data were collected every 2 minutes.

2.3.3 ATR-FTIR spectra preprocessing

All the spectra were recorded to the background spectra. For the PLS-R model calibration and validation the raw spectra were used since OPUS v 7.0.122 software was set up to manage spectral corrections automatically, according to the value of its optimization criteria. For the Kruskal Wallis analysis the raw spectra were corrected for ambient CO_2 only and smoothed. For the multivariate analysis, the raw spectra were corrected for ambient CO_2, smoothed and a second derivative calculation was also performed. All these treatments were achieved using integrated functions of (Bruker Optics, Germany)

2.3.4 Qualitative Multivariate analysis of ATR-FTIR spectra

Pre-processed spectra or pre-processed second derivative spectra were exported as text files for file format modification on Microsoft Excel v14.0.0 or statistical treatment on R 2.15.2. Second derivative spectra were systematically used to improve the infrared band resolution and thus enhance the discrimination of vibrators contributing to the shape of raw FTIR spectra (Mecozzi, Pietroletti, & Tornambe, 2011). The spectral data were centered and scaled (mean subtracted and divided by standard deviation) to minimize the unit range influence before performing unsupervised multivariate analysis (Principal Component Analysis (PCA) and Hierarchical Clustering on Principal Components (HC-PC)) using the factominer R package (Lê, Josse & Husson, 2008). The number of classes was determined without a priori by firstly

using the unsupervised multivariate analysis (i.e. PCA). A refined assessment of the clusters was then performed using a Partial Least Square Discriminant Analysis (PLS-DA), conducted on all the wave numbers stemming from the ATR-FTIR spectra. This multivariate approach was used in order to enhance the formation of clusters by using a model of class prediction (for review see Wold, Sjöström, & Eriksson, 2001). The quality of the prediction was characterized by two parameters, $R^2(Y)$ (goodness of the fit) and Q^2 (predictive capability of the model). The clustering capabilities of the PLS-DA model were considered as satisfactory with both $R^2(Y)$ and Q^2 values superior to 0.5 (Westerhuis et al., 2008). The generation of the PLS-DA models was performed in two steps: first the calibration step ($R^2(Y)$ and Q^2), second the validation step named also the cross validation step ($R^2(Y)$int and Q^2int). For the cross validation step, (Westerhuis et al., 2008) latest study indicated clearly that it was important to notice that even with negative Q^2int values, it was still possible to obtain clear separation between classes. The PLS-DA analysis was conducted using the web server analysis pipeline Metaboanalyst 2.0, dedicated to metabolomic data exploitation (Xia, Mandal, Sinenikov, Broadhurst, & Wishart, 2012). For this supervised multivariate analysis ATR-FTIR spectral data were Log10 [1+x] - transformed and Pareto scaled (divided by the square root of the standard deviation) (Van den Berg, Hoefsloot, Westerhuis, Smilde, & Van Der Werf, 2006).

To assess the influence of the water content on the ATR-FTIR spectra of the tested fibres, a Kruskal Wallis Test (non parametric ANOVA) was performed per wave number of the ATR-FTIR raw spectra recorded on a tested fibre for different water contents. As this non parametric version of the ANOVA does not make any assumption on the nature of the underlying distribution (it does not assume the distribution to be normal), it should be less sensitive to the outliers commonly found in FTIR signatures (since the outliers are taken into account). This allowed a better detection of the vibrators impacted by the water uptake (Di Giambattista et al., 2011). P-value beyond significance threshold (0.05) were plotted on raw spectra data in order to visualize impact of water sorption on ATR-FTIR bands.

2.3.5 Quantitative analysis of ATR-FTIR spectra

There are two steps to obtain PLS-R models: the calibration and the validation. Generally two kinds of validation can be performed: the cross validation and the external validation. Usually the calibration and the cross validation are performed in a single step since identical data set is used to perform calculation.

(i) Calibration and cross validation

For the calibration (cross validation) step, the procedure of calculation and selection of the best predictive model was iterative and comprised a loop formed of two steps. Firstly the pre-processed infrared spectra were regressed against the reference value (i.e. for a considered fibre: its water content determined gravimetrically). Secondly a full cross validation of the model was performed by omitting one sample and operating the test in the remaining spectral data set. This procedure allowed finding models with high correlations R^2 and low Root Mean Square Error of Cross-Validation (RMSECV). The infrared data sets used in our study

comprised 11 samples and 5 replicates per sample, i.e. 55 spectra (ASTM Committee E13, 2005).

(ii) External validation

An independent data set was used for the model evaluation (4 samples and 5 replicates per sample, i.e. 20 spectra) in order to obtain highest correlations (i.e. high R^2) and lowest root mean square error of prediction (RMSEP).

3. Results and discussion

3.1 FTIR qualitative analysis of the water uptake effect on the studied fibres

3.1.1 Each model fibre presented its own FTIR fingerprint

The second derivative spectral data were qualitatively analysed using Partial Least Square Discriminant Analysis (PLS-DA) for each model fibres and for three different relative humidities (RH = 10, 50 and 97 %). On figure 1, results indicate that the three fibres are clustered into three distinct groups, clearly associated to each type of fibre (axis 1). Inside each cluster, it is moreover possible to distinguish subgroups according to relative humidity content (axis 2).

The clustering results clearly reveal that each type of fibre could be distinguished according to its FTIR spectrum, exhibiting moreover differences for the three tested relative humidities. Those observations suggest that each fibre presents its own FTIR signature, depending on its proper chemical composition. Indeed, according to the work of Satyanarayana and colleagues (Satyanarayana, Arizaga, & Wypych, 2009) this spectral signature could be directly related to the amount of the constitutive macromolecules (cellulose, hemicelluloses, lignin and pectin) and to the crystallization degree of the cellulose which are both fibre dependent. Moreover, as the chemical make-up and the crystallinity degree of the fibres are known to influence the moisture sorption, the PLS-DA results suggest that each fibre should present its own water diffusion behavior. Taken together all those remarks indicate that the water quantification models should be developed per type of fibres.

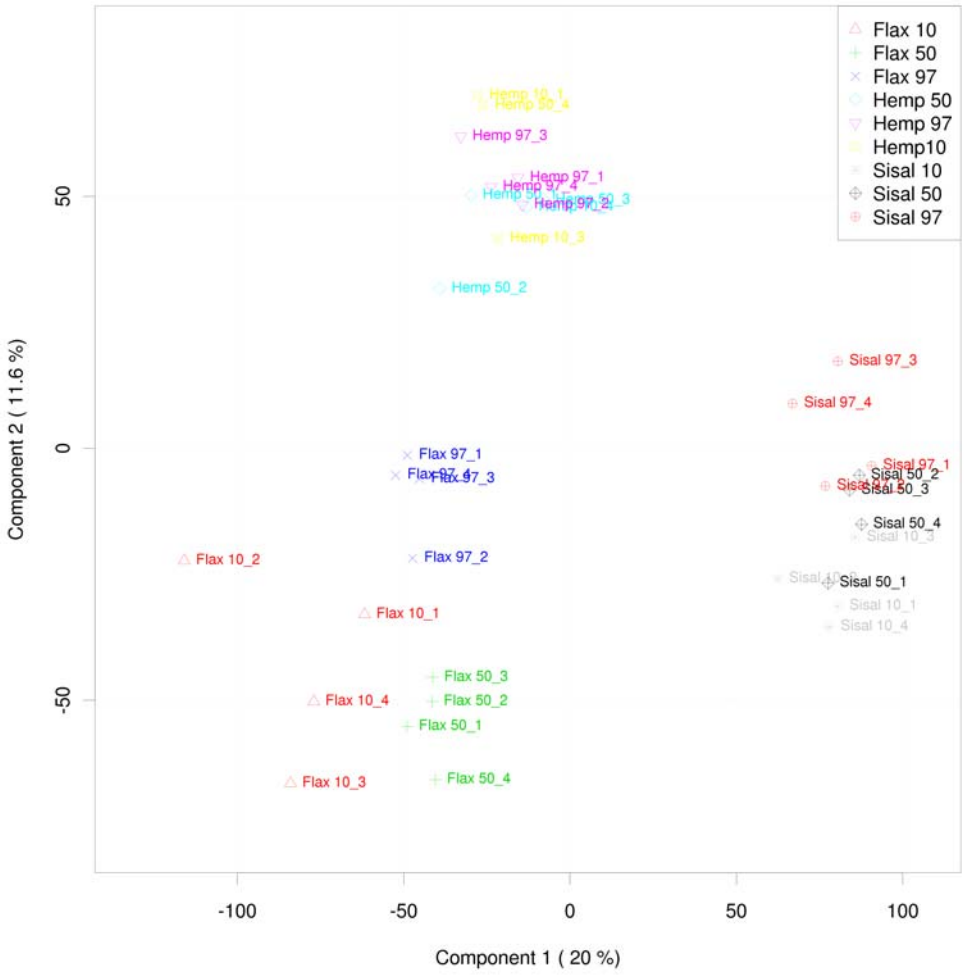

Figure 1: *PLS-DA score plot of second derivative FTIR signatures of the three model fibres for three RH conditions.*
The legend in the upright corner details the nature of the model fibre and the values of the tested RH % (as suffixes). The classification model used here presented the following characteristics i.e. $R^2(Y) = 0,989$ and $Q^2 = 0,869$ and was validated using 20 permutations ($R^2(Y)int = 0,555$ and $Q^2int = -0,343$).

3.1.2 Water sorption molecular sites could be identified for the model fibres subjected to increasing RH %

The spectral dependence on the water content is illustrated on figure 2. The development of the sisal FTIR spectra by increasing relative humidity and water content has been treated here solely for reason of clarity. Similar results were observed for hemp and flax fibres (data not shown). The results of the Kruskal Wallis analysis performed on each individual wave number of the raw spectra highlight several zones of the sisal FTIR fingerprint that were strongly impacted by the increasing water uptake. It helps the FTIR spectra bands assignation (using table 1) and allows the interpretation of the experimental observations.

Table 1: *Assignment of the main absorption bands in FTIR spectra of sisal, flax and hemp fibres. Sisal FTIR data were interpreted according to investigations issued from (Adibi,*

Cabrales, & Haigler, 2013; De Rosa, Kenny, Puglia, Santulli, & Sarasini, 2010; Liang & Marchessault, 1959; Nelsson & O'Connor, 1964).

Wave number (cm^{-1})	Assignment
3600-3100	Hydrogen bonded of OH stretching in cellulose and/or hemicelluloses
2935	CH stretching of cellulose and hemicelluloses
2862	CH_2 stretching of cellulose and hemicelluloses
1735	C=O stretching vibration of carboxylic acid in pectin or ester group in hemicelluloses
1635	OH bending vibration characteristic of sorbed water
1595	Aromatic ring in lignin
1502	Aromatic ring in lignin
1425	Carboxylic acid of pectin and COO- vibration
1375	CH bending of cellulose and hemicelluloses
1335 - 1315	CH_2 wagging of cellulose and hemicelluloses
1275	Characteristic peak of lignin
1240	C-O of acetyl in pectin or hemicelluloses
1160	anti-symmetrical deformation of the C-O-C band
1125-895	C-O stretching and ring vibrational modes
895	Characteristic of β-links in cellulose
700-650	O-H out of plane bending

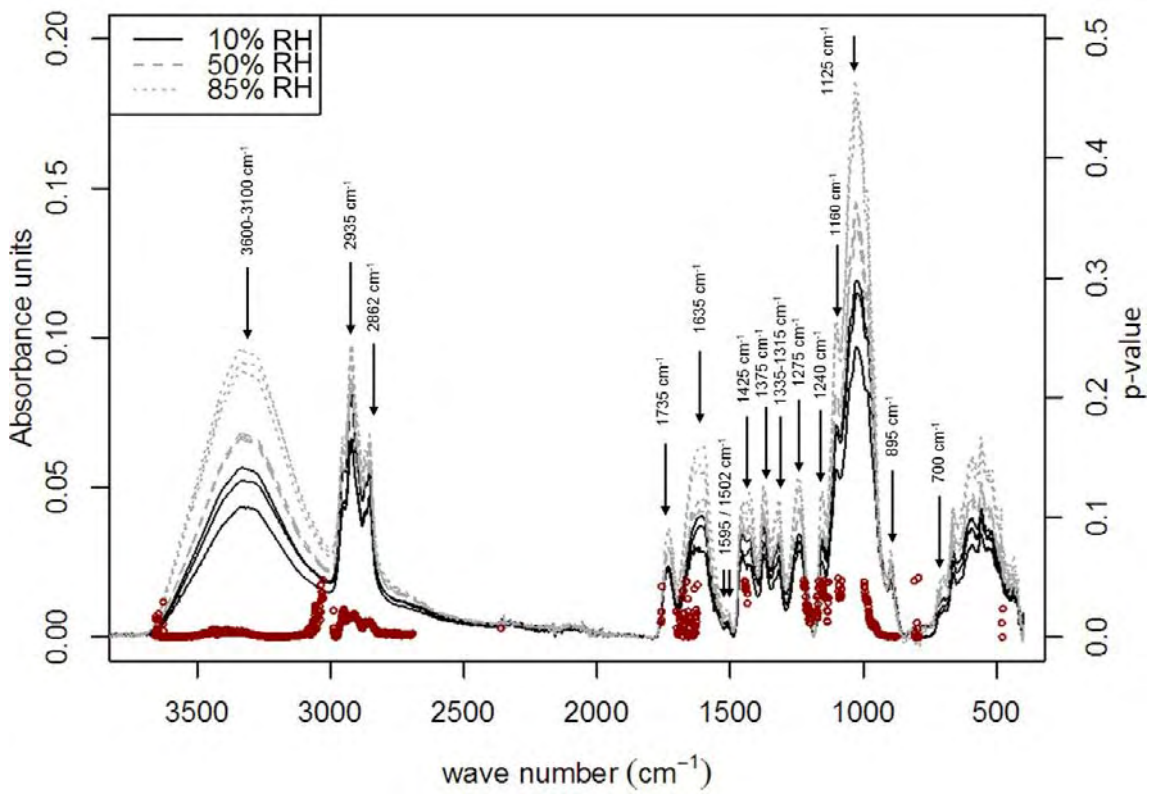

***Figure 2**: Infrared spectra bands impacted by increasing relative humidity for sisal fibre.*

For clarity, only sisal fibre has been presented and only three relative humidities are shown for three replicates (10 %; 50 % and 85 %). p-values scores, indicating significant impact of the water uptake on the FTIR bands, were marked using red dots.

(i) Part of the water-fibre interactions could be associated to the formation of hydrogen bonds between the water and the hydroxyl groups of the cellulose or hemicelluloses constitutive of the raw material.

The broad and unresolved band situated between 3600 and 3000 cm^{-1} was found to be significantly impacted by the increasing relative humidity content. Potential molecular sites of the polymers constituting the studied fibre could be identified here to explain the interactions with the water molecules. Indeed, this band is generally associated to the OH stretching vibrations and hydrogen bonds of hydroxyl groups found in cellulosic materials. However, the absence of clear structured shape makes difficult the assignment of this absorption band (Fengel, 1992; Marchessault, 1962). Recently, (Kondo, 1997) and (Hinterstoisser & Salmèn, 1999) helped its resolution by using fitting deconvolution model and DMA-FTIR coupled analysis, respectively. The hydrogen bonds of hydroxyl groups in the 3600-3000 cm^{-1} wave number range were thus associated to general intramolecular and intermolecular hydrogen bonding and to free hydroxyl in cellulose macromolecule. This peak is also representative of the contribution of the free or the bound water linked to the substrate (Cotugno, Mensitieri, Musto, & Sanguigno, 2005; Murphy & Pinho, 1995; Musto et al., 2000). Here it could be the amorphous phase of the cellulose or the hemicelluloses of the material.

(ii) The water uptake could be also characterized by the monitoring of the interaction between the polymers constituting the raw fibre and the free water.

The interaction of the cellulose or the hemicelluloses molecular sites of sisal, with the free water is also suggested by the significant impact monitored for the FTIR band situated at 1635 cm^{-1}. Indeed such modification was already observed in the case of water diffusion and absorption on cellulosic material, and was found to be characteristic of the free water sorbed on studied material (Laity &Hay, 2000; Murphy & Pinho, 1995). The existence of this interaction should be normally reinforced by the presence of a peak situated at approximately 700 cm^{-1} and assigned to the out of plane bending of the hydroxyl groups characteristic of the free water molecule. However this last peak is not clearly highlighted by the Kruskal Wallis analysis to be dependent of the water content, bringing therefore uncertainty about the influence of free water contribution monitoring. This lack of characterization could be partially explained by the fact that in spectra recorded in attenuated total reflectance, the definition between 700 cm^{-1} and 400 cm^{-1} could not be as good as in transmission mode, precluding therefore the exploitation of the spectral information situated in this range of wave numbers (Parker & Roy, 1966).

(iii) Other molecular sites impacted by the increasing water content could be suggested.

The FTIR bands situated in the wave number interval ranging from 1100 to 700 cm^{-1} were also found to be affected by the water uptake. This signature could be associated to the stretching of the C-O-C group of the polysaccharide components of the studied fibres and

confirmed the previous observation of Olsson and colleagues (Olsson & Salmén, 2004). The evolution of the peak situated at 1425 cm^{-1}could also be associated to the interaction of the water to the carboxylic acid moiety of the pectin polymer as firstly depicted by Marchessault in his exhaustive study on wood polysaccharides infrared spectra (Marchessault, 1962). Surprisingly, according to the Kruskal Wallis p values assignment, the CH stretching bands situated at 2935 and 2900 cm^{-1} were found to be significantly impacted by the water uptake. This is difficult to interpret, since no clear chemical explanation could be envisaged. Several hypotheses could however bring elements of understanding. It could be inherent to the material which is known to be subject to chemical intrinsic variability or be assigned to non-specific experimental variation. Indeed, tests have been performed on different raw fibres for the identical humidities and it effectively highlighted differences in this specific range of wave numbers (data not shown). The way the spectra were processing could also bring elements of explanation. Indeed they were analyzed with almost the same preprocessing treatment than the one used for the PLS-R model generation. In particularly they were not baseline corrected. The shoulder of the OH stretching vibration band clearly shifted up the whole CH bands when the amount of water increases in the sample -whereas no significant increase of the area was monitored (data not shown). This should perturb the Kruskal Wallis test in this particular zone, since it was performed per wave numbers and not per groups of wave numbers –i.e. a band. The combined use of a smoothing function or of moving average performed onto the p values results could enhance the pertinence of the Kruskal Wallis test. These last observations should be carefully considered in the forthcoming multivariate analysis interpretations.

3.1.3 Summary

The results presented above showed that it was possible to discriminate the type of fibre thru its ATR-FTIR second derivative signature using a PLS analysis. Moreover, results revealed that the whole fibre infrared spectra were impacted by the moisture changes. These features strongly suggest that to monitor accurately the water diffusion in the tested biomaterials, a multivariate approach should be used. Indeed, it should improve the water content prediction compared to a univariate approach since the spectral information linked with an increasing water content is visible on the whole spectrum.

3.2 FTIR quantitative analysis of the water content of the studied fibres

3.2.1 It was possible to predict the water uptake of every tested fibre by developing material dependent PLS-R models

The absolute water content of the tested fibres was determined by using a Partial Least Square Regression (PLS-R) approach. For each kind of fibre, the MIR spectra were used in the range from 4000 cm^{-1} to 400 cm^{-1} with the corresponding water uptake measured gravimetrically, to calculate multiple PLS-R models and to perform their validation. The models calculated from the information contained in the spectral regions situated between 3600 cm^{-1} to 3200 cm^{-1} and around 1650 cm^{-1} were selected preferentially since they were associated to the main regions characteristics of the interaction between the water and the polymers constituting each studied fibres (3.1). Other regions were not excluded since they could be associated to the

material intrinsic variability (e.g. around 2900 cm^{-1}). The automatic pre-processing treatments, the spectral regions and the quality indicators (i.e. the cross-validation and the test set validation results) used to calculate the PLS-R models are summarized in the table 2. The spectral regions selected without a priori are in very good agreement with the observations performed in 3.1, especially for the sisal fibre which presents a wave number range distribution correlated to the three main components known to interact with the water molecules. Moreover, the estimation of the errors associated to the predictive models, highlights their pertinence since the RMSECV and RMSEP are very low (≤ to 1). The average number of PLS components is inferior to 7 and the average coefficient of determination greater than 96 %, confirming the quality of the selected models The significance of these parameters has been well described in FitzPatrick and colleagues latest works (FitzPatrick, Champagne & Cunningham, 2012). The figure 3 illustrates the cross-validation and the test set validation results obtained for the sisal fibre. The dispersion diagrams, displaying the relationships between predictive moisture content obtained by PLS-R quantitative model and gravimetric measurements show a very good correlation ($R^2 > 98$).

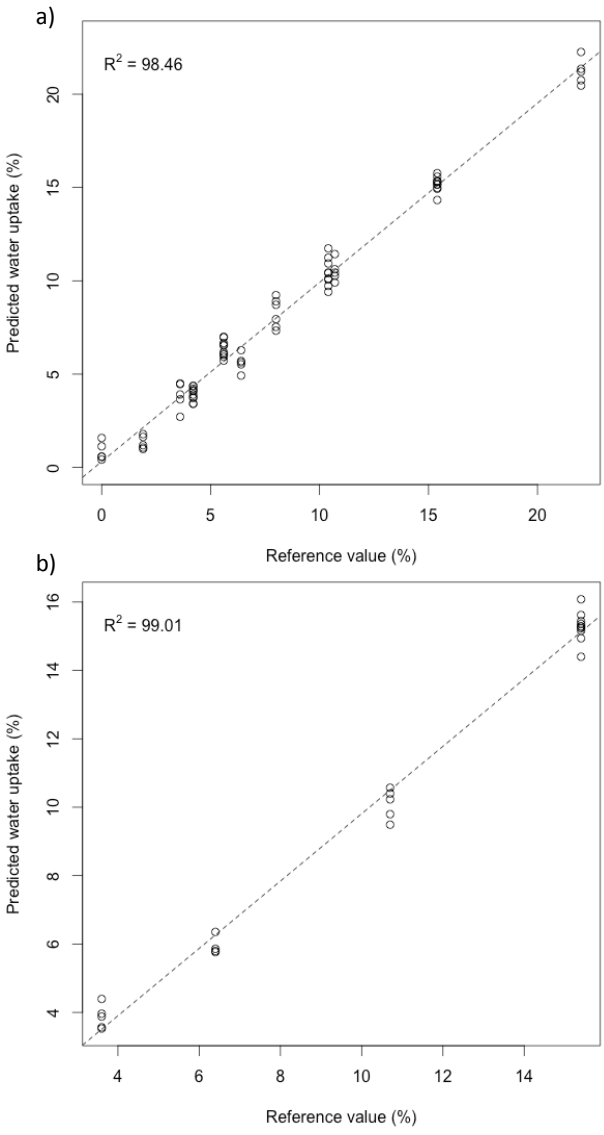

(b)

Figure 3*: Cross-validation (a) and test set validation (b) results of water uptake prediction for sisal fibre.*
The PLS-R predictions of the water content obtained with the FTIR approach were compared here to the gravimetric measurements. The water uptake is expressed in % of the dry weight of the sisal fibre. The coefficients of determination (%) of the regression lines (indicated in dotted lines) are indicated in the upper left corner.

***Table 2**: PLS-R quality parameters for cross and test set validation for the models selected for the three studied fibres.*
RMSECV stands for Root Mean Square Error of Cross Validation. RMSEP stands for Root Mean Square Error of Prediction. R^2 is the coefficient of determination.

		Hemp	Flax	Sisal
	Pre-processing	First derivative	Min/max normalization	Normalization by vector
	Spectral region (cm^{-1})	3998-1119 /760-400	3998-3277 / 2559-2198 / 1839-400	3998-3277 / 1839-1479/ 1120-400
Cross validation	**RMSECV**	1.14	1.07	0,72
	Number of PLS components	4	9	6
	R^2 (%)	95.26	94.92	98.46
External validation	**RMSEP**	0.620	0.843	0,515
	Number of PLS components	5	7	7
	R^2 (%)	97.90	96.65	99.01

3.3 The calculated predictive models were applied to quantify the water sorption phenomenon on the three tested fibres

3.3.1 Monitoring of the sorption isotherm using PLS-R models

The estimation of the water uptake of each studied fibre according to its relative humidity exposition was performed using FTIR spectral information and gravimetric measurements as reference method. FTIR data were interpreted in two ways, one using information arising from one band characteristic of the water sorption (univariate approach) and one exploiting the data of the whole FTIR spectra (multivariate approach: PLS-R model). First, the fibre relative water content was estimated to be solely representative of the absorbance variation of the hydroxyl groups situated in the 3600-3000 cm^{-1} range as already depicted by Olsson & Salmén (2004) (3.1.2). Second, the PLS-R models developed for each studied fibre were used to predict the absolute water uptake taking into account the whole FTIR spectral information. The sorption isotherms present a similar shape for the three studied fibres, whether they were depicted by gravimetric measurements or deduced by FTIR data. The figure 4 illustrates the case of the sisal and indicated that the water content is directly related to the relative humidity by following a sigmoidal relation, as already described by (Alix et al., 2009; Gouanvé, Marais, Bessadok, Langevin & Métayer, 2007). That kind of sorption isotherms are in a good agreement with the Park's model (Park, 1986). This model assumes the association of three mechanisms describing the three parts of the curve (figure 4). It is often used to explain the sorption isotherms of hydrophilic and porous media, as cellulosic fibres (Bessadok et al., 2009).
The first part of the curve could be related to Langmuir's mode (RH < 10 %, this mode is not really visible on the figure 4). At these relative humidities, water is sorbed onto specific sites by hydrogen bonding. As discussed in the section 3.1.2 (qualitative analysis of the bands impacted by water) the specific sites could be hydroxyl functions of amorphous cellulose and hemicelluloses or carboxylic function of pectin. When relative humidity increases, there is a

saturation of these specific sites of sorption. Then, the water concentration increases linearly with relative humidity as Henry's law describes (until RH = 65 %). This behavior could be explained by the porous structure of fibres where water is free to diffuse. The third part is well described by a power function that represents an aggregation phenomenon of water molecules. Indeed, at high relative humidity, water concentration is too important, and water molecules linked together to form clusters.

It is important to notice that the prediction arising from the FTIR PLS-R model fits very well the experimental gravimetric measurements ($R^2 > 99$), highlighting the pertinence of the FTIR multivariate approach compared to the FTIR univariate method ($R^2 < 90$).

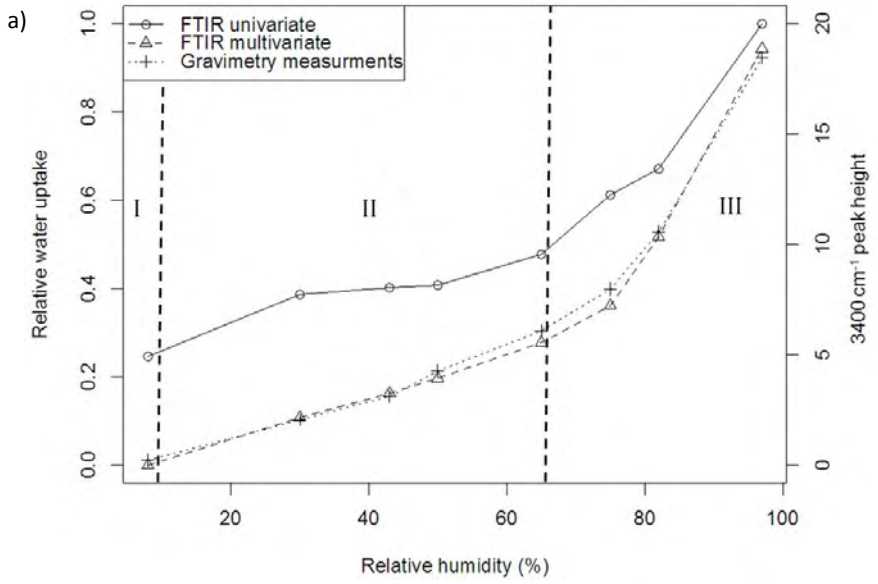

***Figure 4**: Comparison of sorption isotherm for sisal fibre using FTIR and gravimetric approaches. (a) Sorption isotherm plotted for the sisal fibre according to the measurement method (FTIR univariate, FTIR multivariate, gravimetry). (b) Comparison performed between*

normalized FTIR measurements and normalized gravimetric reference method measurements (FTIR univariate-gravimetry: ○, FTIR multivariate-gravimetry :△). R^2 stands for coefficient of determination (%).

3.3.2 Monitoring of the diffusion kinetic using PLS-R models

The desorption kinetics of the water sorbed by the studied fibres were also monitored by exploiting the multivariate FTIR approach. The fibre samples were first aged at RH = 95 % until saturation was reached. Second, FTIR spectra were recorded in kinetic mode during their drying in ambient relative humidity conditions i.e. RH = 45 ± 3 %. FTIR spectral information was treated using the developed PLS-R models for each kind of studied fibres and compared to the gravimetric measurements, systematically performed in parallel. For reason of clarity, the desorption kinetics of sisal fibre is solely represented on figure 5a. FTIR data, predict that after moisture sorption in a wet environment at RH = 95 %, the relative mass gain reached 19 %. This value was correlated with our gravimetric measurements and previous works realized on similar materials (Gouanvé et al., 2007; Stamboulis, Baillie & Peijs, 2001). The desorption kinetic present a sigmoidal shape that could be interpreted as being the consequence of a delay time in the establishment of a water concentration equilibrium at the surface of the studied fibre (similar behaviour was monitored for the others studied fibres (data not shown). At the end of the experiment the initial weight of the fibre was not recovered. A relative mass loss of about 8 %, compared to the initial weight, was observed. Such mass loss could be attributed to the existence of water content in fibres at ambient relative humidity (Baley, Morvan, & Grohens, 2005).

Our experimental data could be well fitted by the Carter and Kibler model as described in Célino and colleagues previous works (Célino et al., 2013). In this model, the moisture absorption is described quantitatively by assuming that the absorbed moisture consisted of both a mobile (i.e. free water) and a bound phase (i.e. bound water). Molecules of the mobile phase should diffuse spontaneously with a concentration and stress independent diffusion coefficient D_γ, and should be absorbed with a probability per unit time γ at certain molecular sites of the polymer fibre. On the other hand, molecules of the bound phase should be released, becoming thereby mobile, with a probability per unit time β. This assumption was supported by the qualitative FTIR spectral data recorded during the diffusion kinetic (figure 5b). Indeed, during the monitoring of the water desorption phenomenon, the main impacted regions (diminishing absorbance) corresponded to the vibration regions of both the free and bound water (3600-3200 cm^{-1}) and the free water uniquely (1635 cm^{-1}) . Those experimental observations strengthen the assumption of the Carter and Kibler model, suggesting that two kind of water population coexisted in the fibres during absorption or desorption. Water should bind to specific sites as hydroxyl or carboxyl functions and free mobile water could diffuse inside the fibre porous structure.

The curve obtained by gravimetric measurement or determined by the PLS-R model based on ATR-FTIR measurement, are in a good agreement. A slight slope difference could be however observed during the transient step. This could be attributed to the fact that the two kinetics were not strictly monitored in identical conditions (section 2.3.2). In gravimetric

measurement, bundle of fibres were free of physical constraints whereas in ATR-FTIR measurements, fibres were pressed above the measurement crystal. The pressure applied by the ATR hammer could accelerate the diffusion of the water from the fibre sample, explaining therefore the observed deviation.

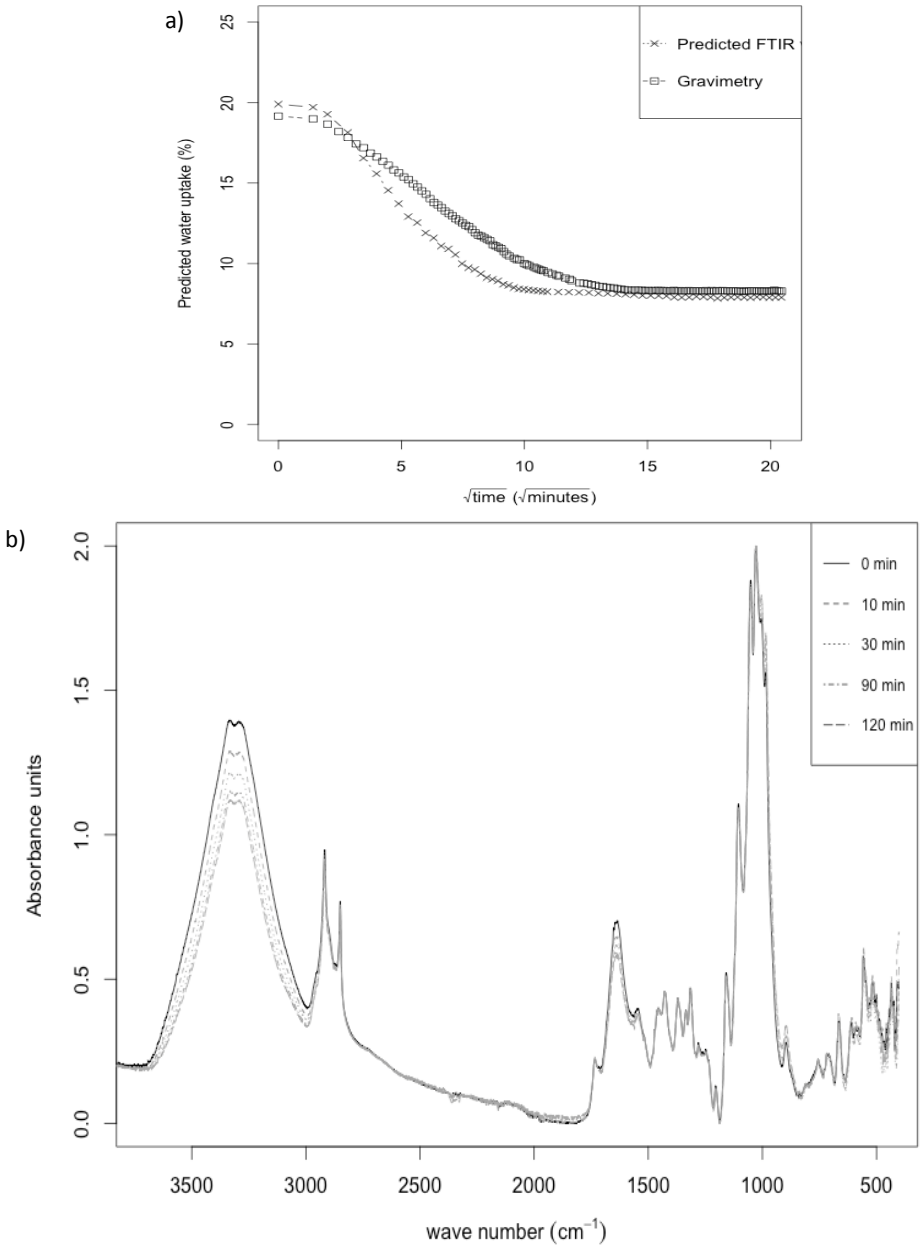

Figure 5: *Quantitative and qualitative monitoring of the water diffusion kinetic for the sisal fibre. (a) Desorption kinetics monitored by FTIR PLS-R prediction and gravimetric approaches. (b) FTIR spectra recorded during kinetic monitoring for time =0, 10, 30, 90 and 120 min.*

4. Conclusion

In the emerging field of composite biomaterials, natural fibres promise an immense potential of application. However, their strong hygroscopic behavior requires the understanding of the moisture sorption mechanisms. Their water content is also of great importance since it could

drive the final properties of the composites where they are fitted in. The aim of this work was to develop a quick and easy method based on ATR-FTIR spectroscopy to characterize qualitatively and quantitatively the water sorption phenomenon directly on raw fibres.

First, our results indicated that it was necessary to develop an approach per fibre since the three tested biomaterials presented their own FTIR signature and therefore their own chemical fingerprint. Hydroxyl and carboxyl molecular sites of the fiber polymer were found to be directly impacted by the water uptake, and confirmed the results observed with less structured cellulosic material (Berthold et al., 1998, Olsson & Salmén, 2004). Second, the FTIR PLS-R models developed for each fibre, in order to quantify their water content, showed very good predictive abilities when compared to the reference method (gravimetric measurements). They were used to monitor accurately sorption isotherms whereas univariate FTIR models could not fit it correctly as depicted by Olsson and colleagues (Olsson & Salmén, 2004). The proposed approach could also supply readily interpretable kinetic data by monitoring continuously the water desorption. The main advantage is the interpretation of kinetics at the molecular level by studying the impacted spectral bands. More detailed analysis (deconvolution of the OH valency band) could lead to the discrimination of the free and the bound water as described in Cotugno and colleagues previous work on an epoxy system (Cotugno et al., 2005).

Moreover, our results indicated that the information collected at the surface of the fibre could be efficiently correlated to a global method based on volumetric measurements (i.e. gravimetry). The multivariate approach used to characterize the water sorption dynamically or statically could explain the quality of the results and should encourage the use of such a direct and rapid approach for water sorption mechanism study on other cellulosic biomaterials.

References:

ASTM Committee E13 on Molecular Spectroscopy and Chromatography. (2005). Standard practices for infrared multivariate quantitative analysis. E 1655-05, 1-29.

Adibi, N., Cabrales, L., & Haigler, C.H. (2013). Changes in the cell wall and cellulose content of developing cotton fibers investigated by FTIR spectroscopy. *Carbohydrate Polymers. In press.*

Alix, S., Philippe, E., Bessadok, A., Lebrun, L., Morvan, C., & Marais, S. (2009). Effect of chemical treatments on water sorption and mechanical properties of flax fibres. *Bioresource and Technology*, *100*, 4742-4749.

Baley, C., Morvan, C., & Grohens, Y. (2005). Influence of absorbed water on the tensile strength of flax fibers. *Macromolecules Symposium*, *222*, 195-202.

Berthold, J., Olsson, R.J.O., & Salmén, L. (1998). Water sorption to hydroxyl and carboxylic acid groups in Carboxymethylcellulose (CMC) studied with NIR-spectroscopy. *Cellulose*, *5*, 280-298.

534 Bessadok, A., Langevin, D., Gouanvé, F., Chappey, C., Roudesli, S., & Marais, S. (2009).
535 Study of water sorption on modified Agave fibres. *Carbohydrate Polymers, 76*, 74–85.
536
537 Bledzki, A.K., & Gassan, J. (1999). Composites reinforced with cellulose based fibres,
538 *Progress in Polymer Science, 24*, 221–274.
539
540 Célino, A., Fréour, S., Jacquemin, F., & Casari, P. (2013). Characterization and modeling of
541 the moisture diffusion behaviour of natural fibres. *Journal of Applied Polymer Science, In*
542 *press.* DOI: 10.1002/app.39148.
543
544 Chalmers, J.M., & Dent, G. (1997). Industrial Analysis with Vibrational Spectroscopy, RCS.
545
546 Cotugno, S., Larobina, D., Mensitieri, G., Musto, P., & Ragosta, G. (2001). A novel
547 spectroscopic approach to investigate transport processes in polymers: the case of water
548 epoxy system. *Polymer, 42*, 6431-6438.
549
550 Cotugno, S., Mensitieri, G., Musto, P., & Sanguigno, L. (2005). Molecular interactions in and
551 transport properties of densely cross linked networks: a time resolved FTIR spectroscopy
552 investigation of the epoxy/H2O systems. *Macromolecules, 38*, 801-811.
553
554 De Rosa, I.M., Kenny, J.M., Puglia, D., Santulli, C., & Sarasini, F. (2010). Morphological,
555 thermal and mechanical characterization of okra (Abelmoschus esculentus) fibres as potential
556 reinforcement in polymer composites. *Composite Science and Technology, 70*, 116-122.
557
558 Di Giambattista, L., Pozzi, D., Grimaldi, P., Gaudenzi, S., Morrone, S., & Castellano, A. C.
559 (2011). New marker of tumor cell death revealed by ATR-FTIR spectroscopy. *Analytical and*
560 *Bioanalytical Chemistry, 399*, 2771-2778.
561
562 Dhakal, H.N., Zhang, Z.Y., & Richardson, M.O.W. (2007). Effect of water absorption on the
563 mechanical properties of hemp fibre reinforced unsaturated polyester composites, *Composite*
564 *Science and Technology, 67*, 1674–1683.
565
566 Feng, J., Berger, K.R., & Douglas, E.P. (2004). Water vapor transport in liquid crystalline
567 and non-liquid crystalline epoxies. *Journal of Materials Science, 39*, 3413-3423.
568
569 Fengel, D. (1992). Characterization of Cellulose by Deconvoluting the OH Valency Range in
570 FTIR Spectra. *Holsforshung, 46*, 283-288.
571
572 Fieldson, G.T., & Barbari, T.A. (1993). The use of FTIR-ATR spectroscopy to characterize
573 penetrant diffusion in polymers. *Polymer, 34*, 1146-1153.
574
575 FitzPatrick, M., Champagne, P., & Cunningham, M. (2012). Quantitative determination of
576 cellulose dissolved in 1-ethyl-3-methylimidazolium acetate using partial least squares
577 regression on FTIR spectra. *Carbohydrate Polymers, 87*, 1124-1130.
578
579 Gouanvé, F., Marais, S., Bessadok, A., Langevin, D. &, Métayer, M. (2007). Kinetics of
580 water sorption in flax and PET fibers. *European Polymer Journal, 43*, 586–598.
581
582 Griffiths, P.R., & Haseth, J.A. (2007). Fourier Transformed Infrared Spectrometry (pp.321-
583 329), Second edition. John Wiley & Sons, Inc.

Hinterstoisser, B., & Salmén, L. (1999). Two-dimensional step-scan FTIR: a tool to unravel the OH-valency-range of the spectrum of Cellulose I. *Cellulose 6*, 251-263.

Kondo, T. (1997). The assignment of IR absorption bands due to free hydroxyl groups in cellulose. *Cellulose, 4*, 281-292.

Laity, P.R., & Hay, J.N. (2000). Measurement of water diffusion through cellophane using attenuated total reflectance-fourier transform infrared spectroscopy. *Cellulose, 7*, 387-397.

Liang, C.Y., & Marchessault, R.H. (1959). Infrared spectra of crystalline polysaccharide. I. Hydrogen bonds in native cellulose. *Journal of Applied Polymer Science, 39*, 269-278.

Lê, S., Josse J., & Husson, F. (2008). FactoMineR: A R Package for Multivariate Analysis. *Journal of Statistical Software, 25*, 1-18.

Marchessault, R.H. (1962). Application of infra-red spectroscopy to cellulose and wood polysaccharides. *Pure Applied Chemistery, 5*, 107-130.

Mecozzi, M., Pietroletti, M., & Tornambe, A. (2011). Molecular and structural characteristics in toxic algae cultures of Ostreopsis ovata and Ostreopsis spp. evidenced by FTIR and FTNIR spectroscopy. *Spectrochimica Acta Part A: Molecular and Biomolecular Spectroscopy, 78*, 1572-1580.

Mijovic, J., & Zhang, H. (2003). Local dynamics and molecular origin of polymer network-water interactions as studied by broadband dielectric relaxation spectroscopy, FTIR and molecular simulations. *Macromolecules, 36*, 1279-1288.

Musto, P., Ragosta, G., & Mascia, L. (2000). Vibrational spectroscopy evidence for the dual nature of water sorbed into epoxy resins. *Chemistery of Material, 12*, 1331-1341.

Murphy, D., & Pinho, M.N. (1995). An ATR-FTIR study of water in cellulose acetate membranes prepared by phase inversion. *Journal of Membrane Science, 106*, 245-257.

Nelsson, M.L., & O'Connor, R.T. (1964). Relation of Certain Infrared Bands to Cellulose Crystallinity and Crystal Lattice Type. Part I. Spectra of Lattice Types I, 11, I11 and of Amorphous Cellulose. *Journal of Applied Polymer Science, 8*, 1311-1324.

Olsson, A.M., & Salmén, L. (2004). The association of water to cellulose and hemicelluloses in paper examined by FTIR spectroscopy. *Carbohydrate Research, 339*, 813-818.

Park, G. S. (1986). Transport principles: Solution, diffusion and permeation in polymer membranes. In P. M. Bungay et al. (Eds.). Synthetic membranes: Science, engineering and applications (57). Holland: Reidel Pub.

Parker, F.S. & Roy, A. (1966). Infrared spectra of carbohydrates (700 – 250 cm^{-1}) determined by both Attenuated Total Reflectance and Transmission techniques. *Applied Spectroscopy, 20*, 384-388.

Placet, V., Cisse, O., & Boubakar, L. (2012). Influence of environmental relative humidity on the tensile and rotational behaviour of hemp fibres. *Journal of Materials Science, **47**,* 3435–3446

Popineau, S., Rondeau-Mouro, C., Sulpice-Gaillet, C., & Martin E.R.S. (2005). Free/bound water absorption in an epoxy adhesive. *Polymer, 46,* 10733-10740.

Satyanarayana, K.G., Arizaga, G.G.C., & Wypych, F. (2009). Biodegradable composites based on lignocellulosic fibers - An overview. *Progress in Polymer Science, 34,* 982–1021.

Stamboulis, A., Baillie, C.A., & Peijs, T. (2001). Effect of environmental conditions on mechanical and physical properties of flax fibres. *Composites Part A, 32,* 1105-1115.

Suddell, B.C., & Evans, W.J. (2005). Natural Fiber Composites in Automotive Applications. In Mohanty, A.K., Misra, M. & Drzal, L.T. (Eds.), Natural Fibers in Biopolymers & Their BioComposites (pp. 231-259). CRC Press.

Summerscales, J., Dissanayake, N.P.J., Virk, A.S., & Hall, W. (2010). A review of bast fibres and their composites. Part I-Fibres as reinforcements. *Composites : Part A, 41,* 1329-1335.

Symington, M.C., Banks, W.M., David, W.O, & Pethrick, R.A. (2009). Tensile Testing of Cellulose Based Natural Fibers for Structural Composite Applications. *Journal of Composite Materials, 43,* 1083-1108.

Van den Berg, R. A., Hoefsloot, H. C., Westerhuis, J. A., Smilde, A. K., & Van Der Werf, M. J. (2006). Centering, scaling, and transformations: improving the biological information content of metabolomics data. *BMC Genomics, 7,* 142-153.

Wambua, P., Ivens, J., & Verpoest, I. (2003). Natural fibres: can they replace glass in fibre reinforced plastics? *Composite Science Technology, 63,* 1259–1264.

Westerhuis, J. A., Hoefsloot, H. C. J., Smit, S., Vis, D. J., Smilde, A. K., Velzen, E. J. J., John P. M., van Duijnhoven, Ferdi A. van Dorsten. (2008). Assessment of PLSDA cross validation. *Metabolomics, 4,* 81-89.

Wold, S., Sjöström, M., & Eriksson, L. (2001). PLS-regression: a basic tool of chemometrics. *Chemometrics and Intelligent Laboratory Systems, 58,* 109-130.

Xia, J., Mandal, R., Sinelnikov, I.V., Broadhurst, D., & Wishart, D.S. (2012). MetaboAnalyst 2.0-a comprehensive server for metabolomic data analysis. *Nucleic Acids Research, 40,* 127-133.

Xie, Y., Hill, C.A.S., Jalaludin, Z., Curling, S.F., Anandjiwala, R.D., Norton , A.J. & Newman, G. (2011). The dynamic water vapour sorption behaviour of natural fibres and kinetic analysis using the parallel exponential kinetics model. *Journal of Material Science, 46,* 479-489.

List of figures

Figure 1: PLS-DA score plot of second derivative FTIR signatures of the three model fibres for three RH conditions.

The legend in the upright corner details the nature of the model fibre and the values of the tested RH % (as suffixes). The classification model used here presented the following characteristics i.e. $R^2(Y) = 0,989$ and $Q^2 = 0,869$ and was validated using 20 permutations ($R^2(Y)int = 0,555$ and $Q^2int = -0,343$).

Figure 2: Infrared spectra bands impacted by increasing relative humidity for sisal fibre.
For clarity, only sisal fibre has been presented and only three relative humidities are shown for three replicates (10 %; 50 % and 85 %). p-values scores, indicating significant impact of the water uptake on the FTIR bands, were marked using red dots.

Figure 3: Cross-validation (a) and test set validation (b) results of water uptake prediction for sisal fibre.
The PLS-R predictions of the water content obtained with the FTIR approach were compared here to the gravimetric measurements. The water uptake is expressed in % of the dry weight of the sisal fibre. The coefficients of determination (%) of the regression lines (indicated in dotted lines) are indicated in the upper left corner.

Figure 4: Comparison of sorption isotherm for sisal fibre using FTIR and gravimetric approaches. (a) Sorption isotherm plotted for the sisal fibre according to the measurement method (FTIR univariate, FTIR multivariate, gravimetry). (b) Comparison performed between normalized FTIR measurements and normalized gravimetric reference method measurements (FTIR univariate-gravimetry: ○, FTIR multivariate-gravimetry :△). R^2 stands for coefficient of determination (%).

Figure 5: Quantitative and qualitative monitoring of the water diffusion kinetic for the sisal fibre. (a) Desorption kinetics monitored by FTIR PLS-R prediction and gravimetric approaches. (b) FTIR spectra recorded during kinetic monitoring for time =0, 10, 30, 90 and 120 min.

List of tables

Table 1: Assignment of the main absorption bands in FTIR spectra of sisal, flax and hemp fibres. Sisal FTIR data were interpreted according to investigations issued from (Adibi, Cabrales, & Haigler, 2013; De Rosa, Kenny, Puglia, Santulli, & Sarasini, 2010; Liang & Marchessault, 1959; Nelsson & O'Connor, 1964).

Table 2: PLS-R quality parameters for cross and test set validation for the models selected for the three studied fibres.
RMSECV stands for Root Mean Square Error of Cross Validation. RMSEP stands for Root Mean Square Error of Prediction. R^2 is the coefficient of determination.

HIGHLIGHTS

- Effect of moisture sorption on plant fibres was investigated by FTIR spectroscopy.
- Hydroxyl and carboxyl moieties are specific sites for water sorption.
- Partial least squares regression quantified the water content of natural fibres.
- Models fitted the sorption isotherms and diffusion kinetics.